We are IntechOpen, the world's leading publisher of Open Access books Built by scientists, for scientists

4,800
Open access books available

122,000
International authors and editors

135M
Downloads

Our authors are among the

154
Countries delivered to

TOP 1%
most cited scientists

12.2%
Contributors from top 500 universities

WEB OF SCIENCE™

Selection of our books indexed in the Book Citation Index in Web of Science™ Core Collection (BKCI)

Interested in publishing with us?
Contact book.department@intechopen.com

Numbers displayed above are based on latest data collected.
For more information visit www.intechopen.com

Chapter 3

Porous Ceramics

Naboneeta Sarkar and Ik Jin Kim

Additional information is available at the end of the chapter

http://dx.doi.org/10.5772/61047

Abstract

The unique chemical composition and microstructure of porous ceramics enable the ceramic products used in a number of applications such as filtration of molten metals and hot corrosive gases, high-temperature thermal insulation, support for catalytic reactions, filtration of diesel engine exhaust gases, etc. These applications take advantage of special characteristics of porous ceramics such as low thermal mass, low thermal conductivity, controlled permeability, high surface area, low density, and high specific strength. In this chapter, we emphasize on direct foaming method, a simple and versatile approach that allows fabrication of porous ceramics with tailored microstructure along with distinctive properties. Foam stability is achieved upon controlled addition of amphiphiles to the colloidal suspension, which induce in situ hydrophobization, allowing the wet foam to resist coarsening upon drying and sintering.

Keywords: Porous ceramics, direct foaming, wet foam stability, Laplace pressure, adsorption free energy, microstructure

1. Introduction

Porous ceramics are widely used in various versatile applications, such as liquid gas filters, catalysis supports, gas distributors, insulators, preforms for metal-impregnated ceramic metal composites, and implantable bone scaffolds [1, 2]. Unlike in metallic or polymeric products, pores have been traditionally avoided in ceramic components because of their inherently brittle nature [3, 4]. However, porous ceramics have become increasingly essential, especially for use in environments involving high temperatures, extensive wear and corrosive media [5,

INTECH
open science | open minds

© 2015 The Author(s). Licensee InTech. This chapter is distributed under the terms of the Creative Commons Attribution License (http://creativecommons.org/licenses/by/3.0), which permits unrestricted use, distribution, and reproduction in any medium, provided the original work is properly cited.

6]. Porous ceramics are advantageous in such application areas due to their high melting point, tailored electronic properties, and high corrosion and wear resistance, which combine favorably with the features gained by the introduction of voids into the solid material [7-10]. These features include low thermal conductivity, controlled permeability, high surface area, low density, high specific strength, and low dielectric constant. These properties can be tailored for each specific application by controlling the composition and microstructure of the porous ceramic. Changes in open and closed porosity, pores' size distribution, and pores' morphology can greatly affect a material's properties. These microstructural features are highly influenced by the processing route used to produce the porous material [11-15].

Foaming melts by gas injection creates gas bubbles in the liquid by the admixing of gas-releasing blowing agents into the molten metal, or by causing the precipitation of gas which had been previously dissolved in the liquid [16, 17]. The stabilization of such foams can be achieved by surfactants, which form dense monolayers on foam films. The surfactant films can reduce surface tension, increase surface viscosity, and create electrostatic forces to prevent foam from collapsing. The stabilization and destabilization mechanisms of coated bubbles exposed to surfactants to produce metallic foams are discussed elsewhere [18]. Colombo et al. [19] discussed different novel processing methods for cellular ceramics, including the burning out of fugitive pore formers. Established methods of producing porous ceramics employ the burning out of templates. The impregnating of a polymeric template increases struts throughout the material and thus increased the strength of the resulting ceramic foams [20]. The porosity of ceramics produced in this way depends on the template's type, content, and grain size. This limits the maximum useable content of such additives, as too high contents substantially weaken the material. Increased porosity can also be achieved by introducing high-porosity granules—both natural (e.g., diatomite, tripolite, and swelled perlite) and synthesized (e.g., by the crushing of briquettes prepared by foaming) [21]. Chemical formations of gas bubbles within a ceramic mixture can also increase porosity. These include chemical reactions in the ceramic suspension or the decomposition of gas-forming additives. The kinetics of alumina slip swelling for the production of lightweight corundum materials have been investigated [22]. Another method is the impregnation of a polymer cellular matrix with a ceramic suspension and subsequent squeezing out, drying, and thermal treatment to remove the organic components [23]. The addition or embedding of ceramic fibers into the mixture, followed by molding with binders and the subsequent thermal treatment of the molded products, can also yield porous materials [24].

The introduction of air into a colloidal suspension is widely used during processing of highly porous foam ceramics [25, 26]. Uniform, finely cellular foam can be produced by mixing into the ceramic suspension frothing agents that stabilize the resultant three-phase foam. Such cellular structures are preserved under subsequent drying and firing [27]. Much work has sought to develop processing parameters for such syntheses.

Less defective components, as compared with dry processing, have recently been shown to result from the wet processing of powders. It allows better control of the interactions between the powder and the particles and increases the homogeneity of particles' packing in the wet stage, leading to fewer and smaller defects in the final microstructure. This can be achieved

http://dx.doi.org/10.5772/61047

either by consolidating the dispersion medium or by flocculating or coagulating the particles in the liquid medium. Such wet methods have recently been developed to incorporate gaseous phases into ceramic suspensions consisting of ceramic powder, solvent, dispersants, surfactants, and gelling agents. The process has been called direct foaming by the hydrophobization of particles' surfaces; the incorporation of the gaseous phase can result from mechanical frothing, injection of a gas stream, gas-releasing chemical reactions, or solvent evaporation [28]. Its simplicity, low cost, and versatility has made it popular for the manufacture of porous ceramics. Fig. 1 outlines common methods of preparing porous ceramics and their corresponding products' degrees of porosity. The fabrication methods of microporous ceramics currently available can be classified as replica techniques, methods that employ sacrificial templates and direct foaming [29]. Ceramics' microstructures and properties depend on their fabrication method. Therefore, consideration of the methods' cost, simplicity, and versatility is important. Stabilization of the introduced species' surfaces is required to overcome coalescence, Ostwald ripening, and phase separation and can be achieved using lower-energy molecules for droplet formation. These provide steric and electrostatic barriers against coalescence [30]. Early twentieth century works by Ramsden and Pickering showed that solid particles adsorbed at liquid-liquid interfaces can stabilize the resulting Pickering emulsions, through the introduced surface active molecules lowering the system's free energy by reducing the liquid-liquid interfacial area [31].

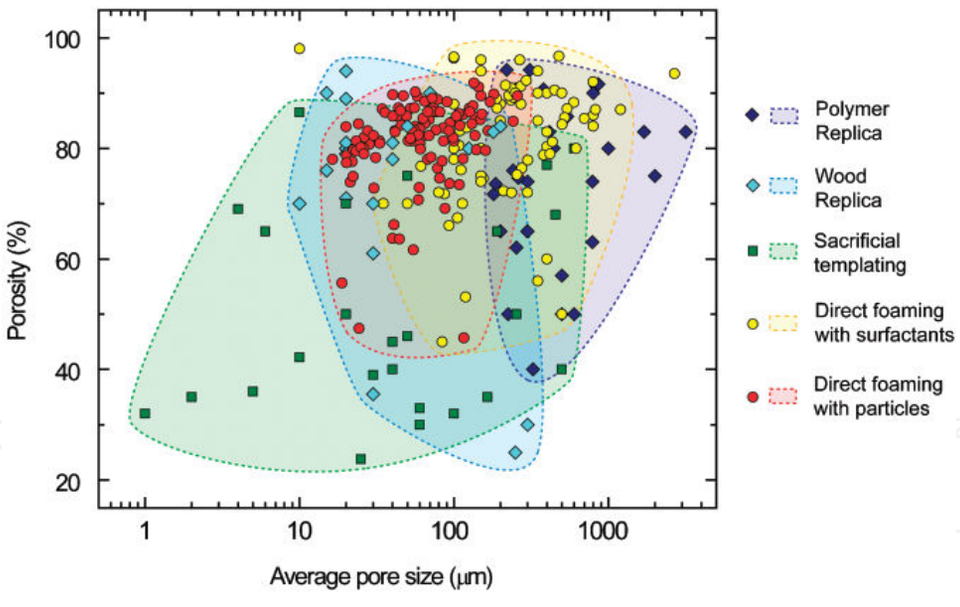

Figure 1. Typical porosity and average pores sizes achieved via replica, sacrificial templating, and direct foaming routes.[2]

This chapter explores the stabilization of wet foams by colloidal amphiphilic particles and the development of fabrication techniques of solid macroporous ceramics with tailored microstructures. Each method is discussed and assessed with regard to the versatility and ease of fabrication and its influence on the microstructure and mechanical strength of the resulting macroporous ceramics. Given the importance of ceramics' foam microstructures, the effects of

foam precursor suspensions—bubble size, distribution, contact angle, and surface tension—on the resultant porous ceramics' mechanical and physical properties are assessed here. Control of these parameters can allow the tailoring of the microstructures of porous ceramics produced by direct foaming.

2. Processing routes to porous ceramics

The processes for manufacturing porous ceramics can be classified into following four categories, which is schematically depicted in Fig. 2.

i. Replica techniques

ii. Sacrificial template

iii. Direct foaming

In this chapter, we reviewed the main processing techniques that can be used for the fabrication of porous ceramics with tailored microstructure. Replica techniques, sacrificial template, and direct foaming techniques is described here and compared in terms of microstructures and mechanical properties that could be achieved. These simple yet versatile approaches give rise to porous ceramics with unique microstructural features that control the properties and functions of the ceramic materials.

2.1. Replica techniques

Replica techniques involve the impregnation of a cellular structure with a ceramic suspension or precursor solution to produce a macroporous ceramic exhibiting a similar morphology to the original porous material (Fig. 2(a)). This is followed by the removal of excess slurry, pyrolysis of the polymeric substrate, and sintering to solidify the foam [6, 13]. Therefore, the ceramic foam replicates the original organic polymer structure. Difficulties of slurry impregnation limit the realization of small cells. The struts contain central holes, which result from the burning out of the polyurethane template. Microcracks and pores also result. Replication generates large amounts of CO_2 during firing due to the decomposition of the organic compounds [10, 12]. Suitable biogenic porous structures have been used as templates to form cellular ceramics with particular microstructures that could also be produced by other methods. Those processes for the fabrication of bulk ceramics structures are discussed here.

This technique, reported in the 1960s, is the first method deliberately used for the production of macroporous ceramics [32]. First, polymeric sponges were used as templates to prepare ceramic cellular structures with various pore sizes, porosities and chemical compositions. In the polymer replica approach, a highly porous polymeric sponge is initially soaked in a ceramic suspension until its internal pores are filled. Binders and plasticizers are also added to the initial suspension to provide ceramic coatings sufficiently strong to prevent the struts from cracking during pyrolysis. This process is explored fully elsewhere [11, 13].

http://dx.doi.org/10.5772/61047

The resulting ceramic is formed after removal of the polymeric template. The ceramic coating is finally densified by sintering at 1000-1700°C depending on the material. Porous ceramics obtained via sponge replication can reach total open porosity levels of 40%-95% and are characterized by a reticulated structure of highly interconnected pores of between 200 μm and 3 mm. The disadvantages of this technique lie in the formation of the struts of the reticulated structure during pyrolysis of the polymeric template, which significantly weakens the mechanical strength of the resulting porous ceramic [21]. The technique also requires several steps, which lengthen its duration and increases its cost.

2.2. Sacrificial templates

A dispersed sacrificial phase can be homogeneously dispersed throughout a biphasic composite with a continuous matrix of ceramic particles or ceramic precursors. It is ultimately extracted to generate pores within the microstructure (Fig. 2(b)). This method is analogously opposite to replication and results in a negative replica of the original sacrificial template, as opposed to the positive morphology obtained from replication. The method of the sacrificial material's extraction from the consolidated composite depends primarily on the type of pore former employed [33]. A wide variety of sacrificial materials can be used as pore formers, including natural and synthetic organics, salts, liquids, metals, and ceramics. This technique is flexible and can employ various chemical compositions. Various oxides have been used to fabricate porous ceramics using starch particles as sacrificial templates [9, 10]. Nonoxide porous ceramics have also been produced using pre-ceramic polymers and various template materials [34, 35]. Since this method produces a ceramic to the negative of the original template, the removal of the sacrificial phase does not lead to flaws in the struts as can occur using positive replicas. The microstructures obtained by this technique reflect directly the pattern of the sacrificial phase and higher mechanical strengths are generally achievable than by using positive replicas [36, 37].

2.3. Direct foaming

Direct foaming produces porous materials by the incorporation of air into a suspension or liquid medium. The foam structure is then set by high-temperature sintering to obtain crack-free, high-strength porous ceramics. The suspensions are stabilized *in situ* through the hydrophobization of the suspended particles by short chain amphiphilic molecules. The coated, hydrophobic particles irreversibly adsorb to the air-water interface, thus stabilizing it (Figs. 2(c) and 3) [38]. These wet foams can remain stable for several days and show no bubble coarsening, drainage, or creaming. The short-chain amphiphiles modify *in situ* the wetting behavior of the particles' surfaces, as in a Pickering emulsion. Ultrastable wet foams can be produced by direct foaming using particles instead of surfactants as foams stabilizers [16, 19, 25]. Porous ceramics' properties are also highly influenced by their chemical compositions and microstructures, with porosity, pore morphology, and size distribution being tailored by different compositions, different physical structures of the starting materials, and the use of different amphiphiles [30-36]. This review focuses on this process.

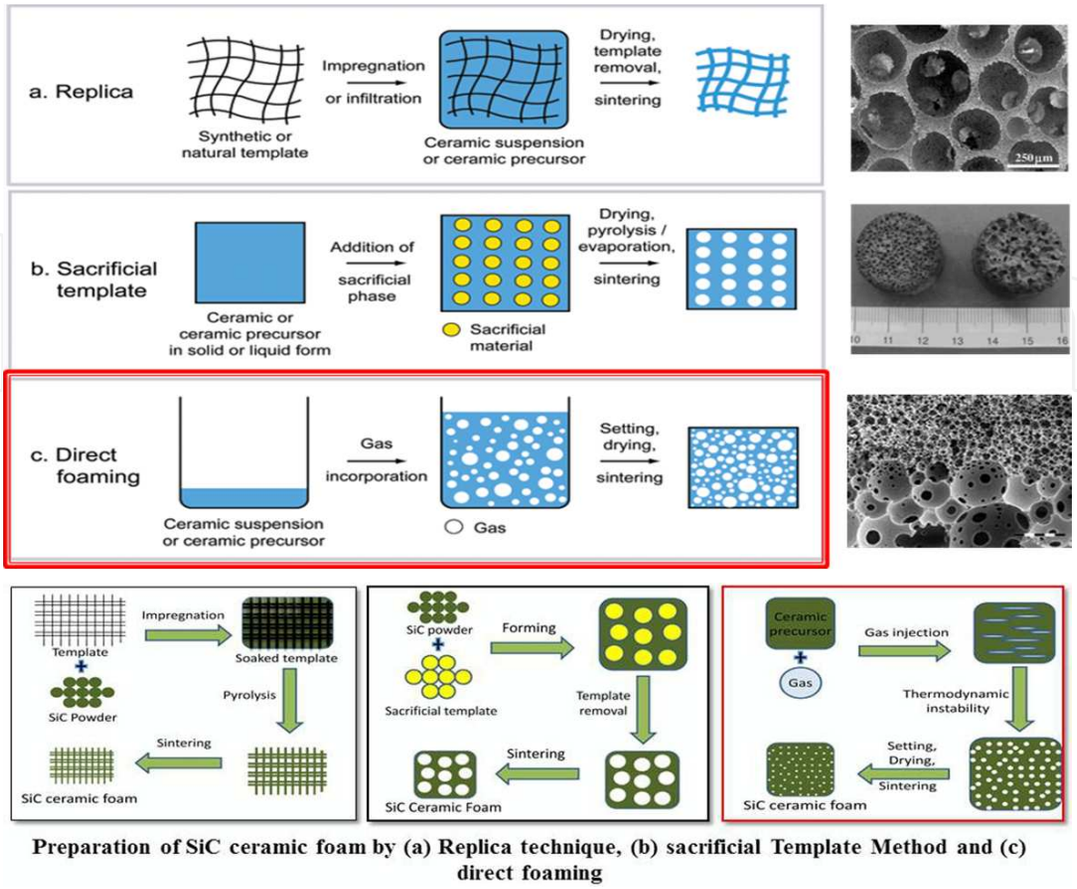

Figure 2. Currently available methods of forming porous ceramics.[2]

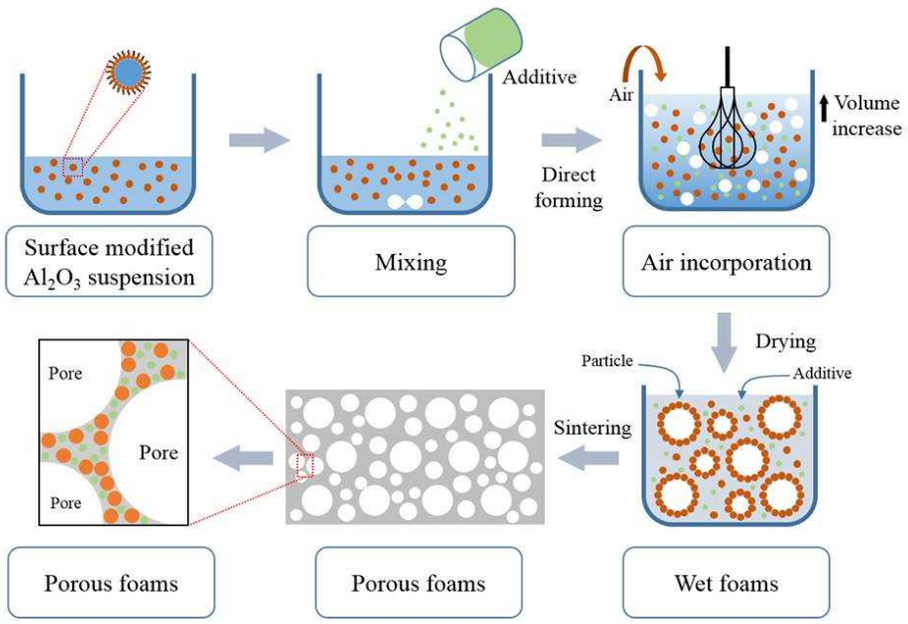

Figure 3. *In situ* hydrophobization of particles and solid foam formation by direct foaming.[4]

http://dx.doi.org/10.5772/61047

3. Process to stabilization

3.1. Zeta potential and *in situ* hydrophobization

Colloids are suspensions or liquid foams that are generally thermodynamically unstable. The instability arises due to their high gas-liquid interfacial areas, which raise the free energy of the system. To achieve a stable system, free energy must be minimized. The electrokinetic properties of a colloidal system can be described using the zeta potential (Figure 4(a)). Higher charges on the particles' surfaces stabilize a colloidal suspension by preventing the particles from coming into contact and coalescing. Colloids with high zeta potential (negative or positive) are electrically stabilized while colloids with low zeta potentials tend to coagulate or flocculate as shown in Table 1. A suspension's pH affects its charge distribution, and hence its zeta potential. The isoelectric point (IEP) is the pH at which a colloid's zeta potential is zero; it can be used to derive information about the pH ranges in which a colloid is stable. A suspension's pH can be modified to allow dissociated surfactant to adsorb electrostatically as counter ions onto oppositely charged alumina hydroxyl surface groups [39]. The suspension's inorganic particles can be stabilized *in situ* by the particles' hydrophobization with different colloidal particles containing predominantly $-OH_2^+$, -OH, and $-O^-$ surface groups. Surfaces with predominantly $-OH_2^+$ and -OH groups can be achieved on inorganic alumina particles at pH 4.5 and pH 9.5, respectively. This could be derived from the zeta potential data for bare alumina particles (Fig. 4(b)), which confirm that the surface exhibits mainly $-OH_2^+$ (positive net charge) and -OH (neutral net charge) groups under those conditions [26, 31, 20]. Amphiphiles of short chain carboxylic acids and gallates are expected to adsorb well onto alumina particles. Propyl gallate has been used to modify the surfaces of particles by ligand exchange reactions [15]. The surface hydroxyl groups (-OH or $-OH_2^+$) were replaced by one or more of the molecule's hydroxyl groups (-OH or $-O^-$). Therefore, the adsorption of gallate molecules does not necessarily require oppositely charged surfaces and amphiphiles and can be used at pH values at which the surface groups and the molecules exhibit the same charge polarity. Hydrophobizing adsorption can change the wettability of particles at the interface of two immiscible phases, and the system is stabilized by the neutral forces between the particles and the amphiphilic coatings. Therefore, the choice of amphiphile depends upon the IEP and the zero net charge of the oxide. Surface hydrophobization can be accomplished by choosing amphiphiles with functional groups that react with the surface hydroxyl groups. Pyrogallol groups can efficiently adsorb on oxide surfaces via ligand exchange reactions [14, 16] and thus can be used with a short hydrocarbon tail to modify the surfaces of particles with intermediate IEPs. The selection of amphiphiles with suitable head groups and tail lengths allows the surface hydrophobization of particles of various compositions.

3.2. Destabilizing suspension

Colloidal dispersions can be thermodynamically unstable, with long-term kinetic stability determining their self-life. The main destabilization mechanisms are drainage (creaming and sedimentation), coalescence, and flocculation (Fig. 5). Creaming and sedimentation are caused by gravity: lighter particles float and heavier particles settle. They are reversible in that

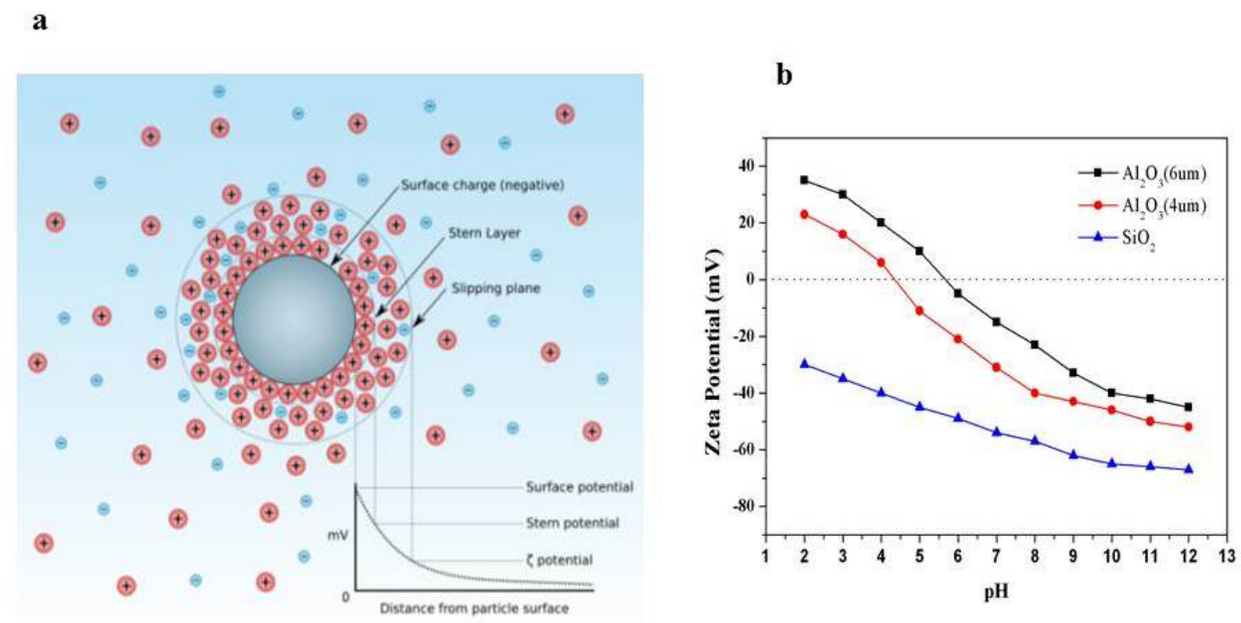

Figure 4. (a) The distribution of charges in a colloidal suspension; higher charges at the particles' surfaces can stabilize the system. (b) Zeta potential of raw Al_2O_3 and SiO_2 colloidal particles.

Zeta potential [mV]	Stability behaviour of the colloid
From 0 to ±5	Rapid coagulation or flocculation
From ±10 to ±30	Incipient instability
From ±30 to ±40	Moderate stability
From ±40 to ±60	Good stability
More than ±61	Excellent stability

Table 1. Zeta potential as key indicator of the stability of colloidal dispersions

mechanical agitation (homogenization or simple shaking) will redisperse the suspension. Coalescence and flocculation are not reversible and so affect a suspension's stability. Flocculation is the clustering of colloidal particles via attractive van der Waals forces. It can be overcome or prevented by higher-energy ultrasonification or by generating particles with repulsive interactions [40]. Coalescence is the greatest destabilizing mechanism. It involves smaller particles collapsing into each other, forming larger particles with different properties. Many dispersion techniques have been developed to prevent coalescence [41].

3.3. Suspension stability

The foams require the adsorption of particles on the surfaces of air bubbles upon their formation. Alumina particles can be hydrophobized by modification with short-chain carboxylic acids: the carboxylate groups adsorb to the alumina's surface [42], leaving the hydrophobic tail in contact with the aqueous solution. This has been shown to stabilize the dispersion [43].

http://dx.doi.org/10.5772/61047

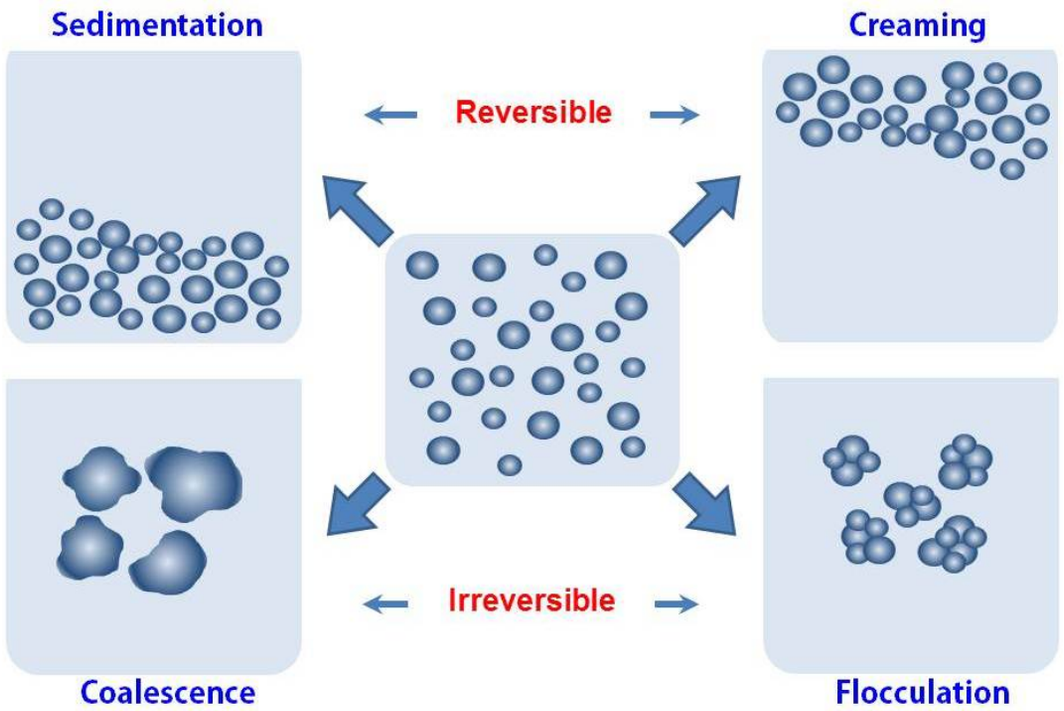

Figure 5. The destabilization of colloidal suspensions.

The hydrophobicity imparted by the first layer of depronated amphiphiles adsorbed onto the surface leads to an energetically unfavorable exposure of hydrophobic species to the aqueous phase. This favors the adsorption of additional molecules from the aqueous phase onto the particles' surfaces to decrease the system's free energy, which determines the stability of a suspension or wet foam. Particles attached to foam and mists' gas-liquid interfaces lower the overall free energy by replacing part of the interfacial area rather than reducing the interfacial tension, as in the case of surfactants [5]. The energy of the attachment, i.e., the Gibbs free energy (G), gained by the adsorption of a particle of radius *r* at the interface can be calculated using simple geometrical arguments that lead to the following equation (Fig. 6).

$$G = \pi r^2 \Upsilon_{LG} \left(1 - \cos\theta\right) \text{ for } \theta < 90^\circ,$$

where θ is the contact angle and $_{LG}$ is the gas-liquid interfacial tension. While the maximum energy gain can only be achieved at $\theta = 90^{\circ}$, contact angles as low as 20º can yield attachment energies in the order of 10^3 kT in systems of 100 nm particles [2]. The high energy associated with the adsorption of particles at interfaces contrasts to low adsorption energies of surfactants and leads to foams stabilized by particles being more stable than those stabilized with surfactants. It also leads to steric layers which strongly hinder bubbles' shrinkage and expansion, minimizing Ostwald ripening for very long periods of time [46].

The particle systems described in Fig. 6 had adsorption achieved by ligand exchange, whereby a surface hydroxyl group is exchanged for another group. This occurred because of the

favorable change in the surface charge by the removal of (OH_2^+), a better leaving group, and replacement with (-OH) [44, 45].

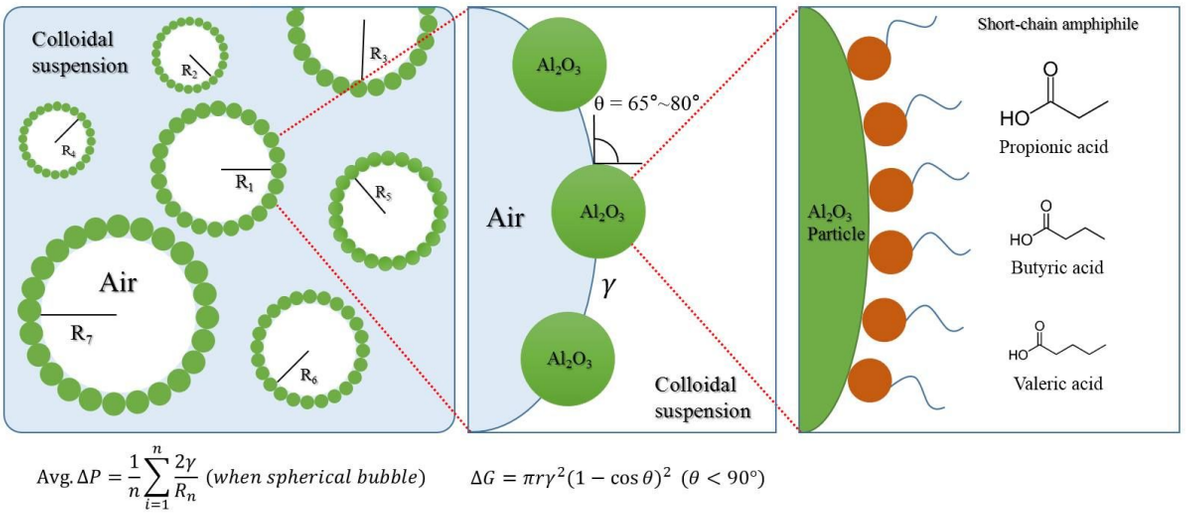

Figure 6. Foams produced through the adsorption of colloidal particles at the gas-liquid interface.

3.4. Contact angle and surface tension

After the stabilizing effects of zeta potential and pH, contact angle and surface tension are important determinants of colloidal systems' properties. Once a suspension is stabilized, the degree of hydrophobization is the main property which affects the production of foam. Given their thermodynamic instability, foams are often kinetically stabilized through the adsorption of surface active molecules or colloidal particles at the gas-liquid interfaces [46, 47]. The adsorbed molecules and particles stabilize the system by inhibiting the coalescence and Ostwald ripening of droplets and bubbles. Adsorption at the fluid interfaces occurs when particles are not completely wetted by any of the fluids, thus exhibiting a finite equilibrium contact angle at the triple phase boundary.

The equilibrium contact angle (θ) is determined by the balancing of the interfacial tensions (Equation 1). A decrease in surface tension upon increasing the initial amphiphile concentration can be observed. However, above a critical amphiphile concentration, surface tension decreased sharply. Above this critical amphiphile concentration, the particles are sufficiently hydrophobic at the air-water interface and decrease surface tension more greatly than that expected from free amphiphiles alone [48]. This significant reduction in surface tension upon particle adsorption was caused by a decrease of the total area of the highly energetic air-water interface. Similar surface tension effects have been observed in systems employing various amphiphiles [18]

Controlling particles' contact angles at the interface is important as it determines their wettability (Fig. 7). Tailoring particles' contact angles via modification of chemical composition

enables the creation of foams with a variety of functionalities [19]. Contact angle depends on surface chemistry, roughness, impurities, particle size, and fluid phase composition. Theoretical and experimental work has shown that stabilization is achieved when contact angles are of an intermediate range of 20-86º for oil-in-water foams and of 94-160º for water in oil foams [49]. Contact angle can also be tailored by changing the particles' surface chemistry or adjusting the composition of the fluids. Metallic and ceramic particles can achieve any contact angle ($0 < \theta < 180º$) by reacting or adsorbing hydrophobic molecules on their surfaces [28, 29]. The use of short amphiphiles to tailor particles' wettability is a general and versatile approach for the surface modification of a wide range of ceramic and metallic materials [20].

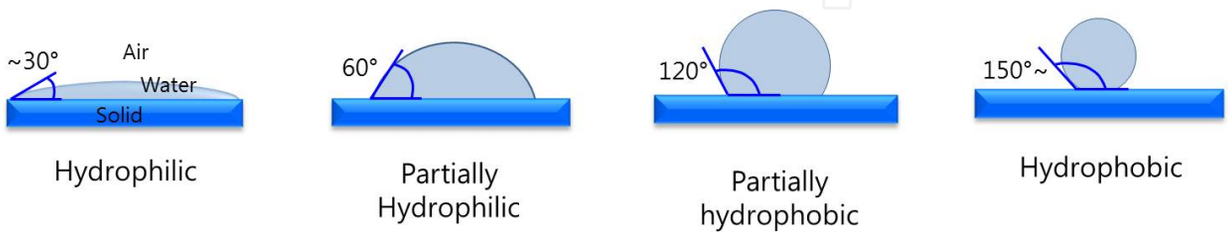

Figure 7. The wettability of particles in immiscible phases.[2]

3.5. Wet foam stability

Liquid foams are thermodynamically unstable due to their high gas-liquid interfacial area. Several physical processes can occur to decrease the overall free energy and destabilize the foam [36]. Drainage occurs through gravity; light gas bubbles rise forming a denser foam layer, while the heavier liquid phase is concentrated below. Coalescence takes place when the thin films formed after drainage is not stable enough to keep adjacent cells apart. Their collapse results in the joining of neighboring bubbles. The stability of the thin films is therefore described in terms of attractive and repulsive interactions between the bubbles. van der Waals forces drive the bubbles closer. They can be overcome by electrostatic forces, steric repulsions force, or ligand exchange reactions. Surfactant or particles adsorbed at the air-water interface can also reduce van der Walls forces [22]. Ostwald ripening or disproportionation is another destabilizing effect that is more difficult to overcome. It occurs due to differences in the Laplace pressures between bubbles of different sizes. Laplace pressure inside a gas bubble arises from the curvature of the air-water interface. The Laplace pressure (N/m^2) is the pressure difference between the inner and the outer side of a bubble or droplet. For spherical bubble of radius R and gas-liquid interfacial energy γ, the Laplace pressure ΔP is given by $2\gamma/R$. The pressure and force generated for the stabilization can be also calculated through the measurement of bubbles at the intersection. It can be calculated by the equation given below.

$$\Delta P = \gamma\left(\frac{1}{R_1} + \frac{1}{R_2}\right) = \frac{2\gamma}{R}\left(\text{spherical bubble}\right)$$

The difference in the Laplace pressure between bubbles of distinct sizes (R) leads to bubble disproportionation and Ostwald ripening because of the steady diffusion of gas molecules from smaller to larger bubbles over time. This process can be slowed by using surfactants or particles adsorbed at the interface, which decrease the interfacial energy. Wet foam's stability is also related to the degree of hydrophobicity achieved from the surfactant, which replaces part of the highly energetic interface area and lowers the free energy of the system, leading to an apparent reduction in the surface tension of the suspension [49]. Stability also depends on surface charge screening, the electrical diffuse layer around a particle's surface not sufficiently thick to overcome the attractive van der Waals forces between particles. Overcoming the van der Waals attractions requires a stable hydrophobizing mechanism (examined above). Therefore, experiments were conducted as per reported theoretical explanations [18].

These actions' combined effects may collapse the foam within minutes after air incorporation. Foams' life times have been increased from several hours to days and months by the adsorption of the short chain amphiphilic molecules [50], while only a few minutes or hours' stabilization results from the use of long-chain surfactants or proteins at the air-water interface [35]. Unlike other particle-stabilized foams [2], these foams percolate throughout the whole liquid phase and exhibit no drainage over days and months [49] due to the high concentration of modified particles in the initial suspension, which allows for the stabilization of very large total air-water interfacial areas.

4. Results and discussions

4.1. Contact angle and surface tension

The attachment of particles at gas liquid interfaces occurs when particles are not completely wetted or, in other words, are partially hydrophobic. This enables the production of high-volume stable foam, which produces porous ceramics after drying and sintering. Partially hydrophobic particles remain predominantly in the liquid phase and exhibit a contact angle <90°. Therefore, controlling contact angles of the particles at the interface is important since the angles modify the wettability of the particles by changing their hydrophobicity, as shown in (Figs. 8-10). Generally, lower contact angles improve the wettability. Different contact angles can be achieved by imparting different hydrophobic molecules commonly known as surfactants.

It is shown from Fig. 8 that the average contact angle of the d_{50} ~ 40 nm Al_2O_3 suspension decreased from 84° to 67° with the increased SiO_2 content (1.0 mole ratios in the Al_2O_3 suspension). Also, the increasing SiO_2 content produced lower adsorption free energy due to the higher interparticle attraction, increasing the viscosity. The suspensions with mol ratios of SiO_2 between 0.25 and 0.5 in the suspension show higher levels of attachment energy, resulting in highly stable foam in the sintered porous ceramics. Also, contact angle of around 70°-75° for the nanoparticle suspension leads to better wet foam stability and can give surface tensions of 21-33 mNm^{-1}. The required partial hydrophobization of the particles occurs at this point, which leads to porous ceramics with higher porosity.

http://dx.doi.org/10.5772/61047

Fig. 9 shows the effect of suspension added for the mullite phase on the contact angle and surface tension of the aqueous suspensions. From this graph, we can see the suspension exhibits contact angles of 46°-55°, which enables high wet foam stability, as that indicates partial hydrophobization of particles has taken place. We observed that for all the evaluated samples, the surface tension of suspensions decreases, upon increasing the vol% of suspension added for the mullite phase. This can be explained by an increase in surface hydrophobicity of the particles with increasing particle concentration.

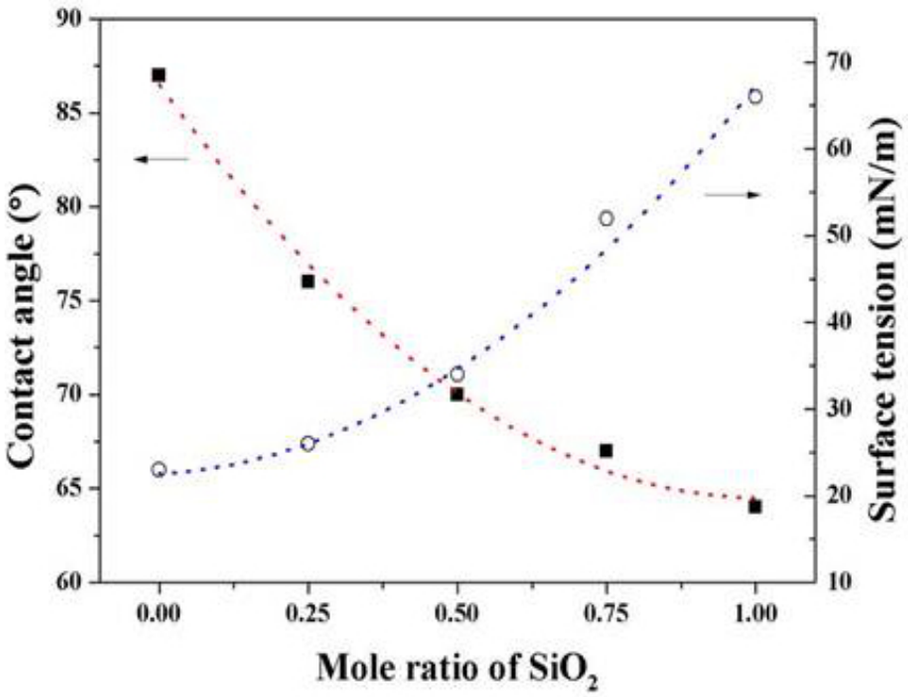

Figure 8. Contact angle and surface tension of colloidal suspension with respect to different mole ratio of SiO_2.

In Fig. 10, the hydrophobization achieved via amphiphile adsorption was confirmed by contact angle measurements of the aqueous suspensions. As we can see, the 0.05-mol/L concentration of propionic acid was not sufficient enough to impart particle hydrophobicity, which results in unstable foams. From this graph, we can conclude that a contact angle of 65°-72° produces required particle hydrophobicity which enables high wet foam stability.

In Fig. 11, the degree of particle hydrophobization achieved by imparting different concentration of amphiphile was investigated with the help of surface tension measurements. The surface tension of suspensions containing 30 vol% particles and different concentration of amphiphiles is shown in Fig. 11. A decrease in surface tension upon increasing the amphiphile concentrations is observed for all the evaluated suspensions. The reduction in surface tension results from the adsorption of free amphiphile molecules to the air-water interface. The middle and short chain amphiphiles, i.e., butyric acid and valeric acid, respectively, impart relatively low surface energy, which enables sufficient hydrophobicity on the particle surface than the shortest chain amphiphile, i.e., propionic acid, does.

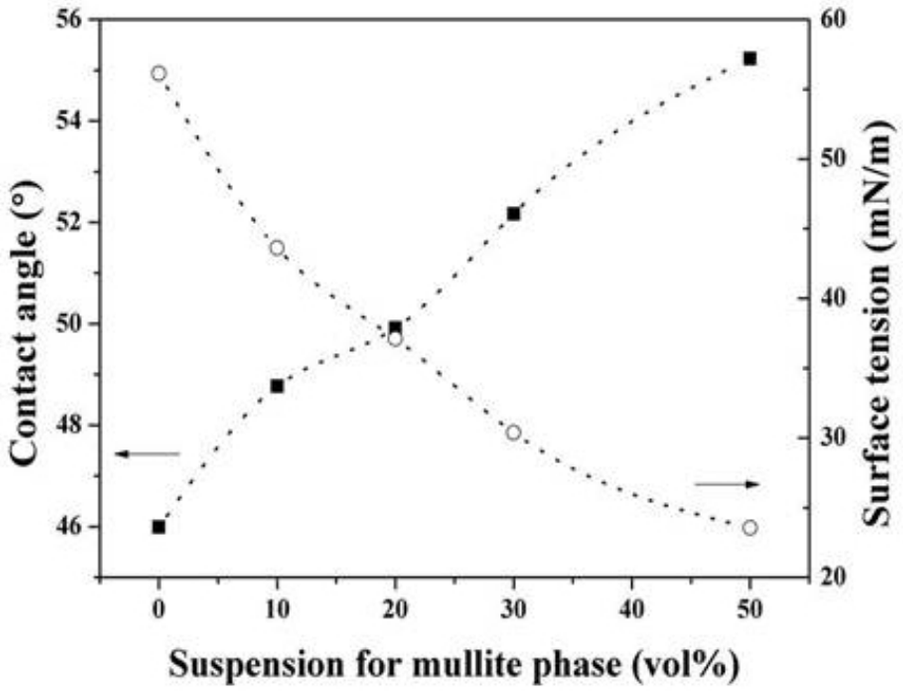

Figure 9. Contact angle and surface tension of Al_2O_3-TiO_2equimolar suspension, with respect to different vol% of 3:2 mole ratio of Al_2O_3-SiO_2 suspension added for the mullite phase[32]

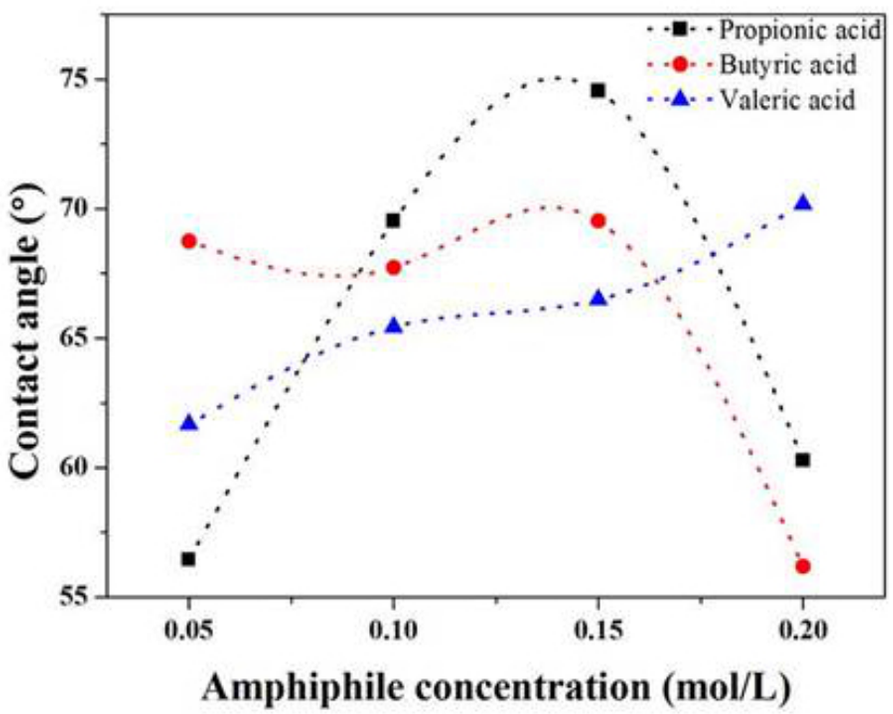

Figure 10. Contact angle of suspension with respect to different concentrations of amphiphiles.[4]

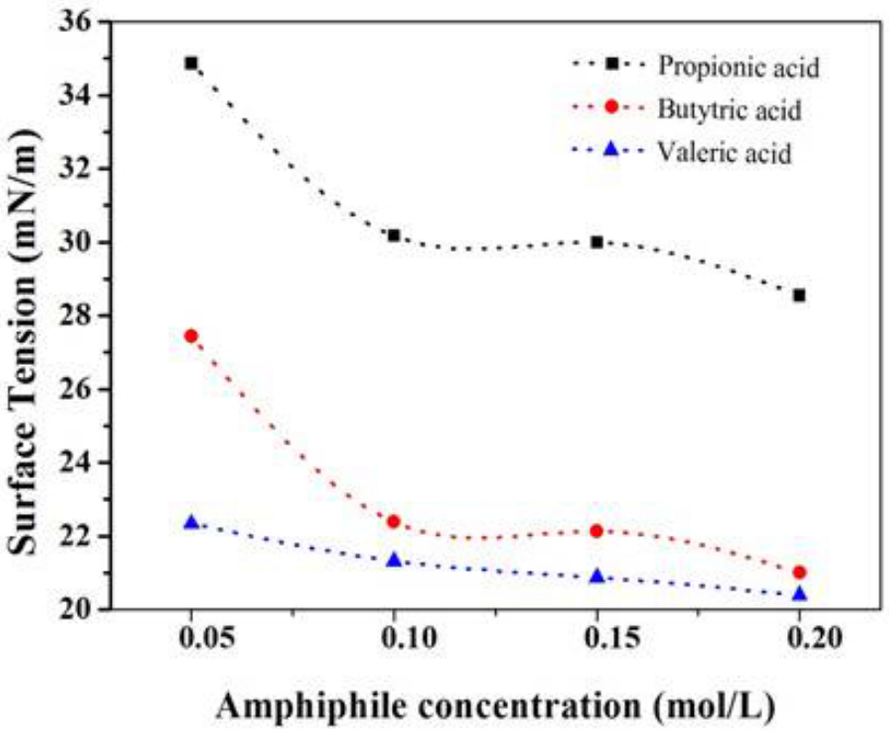

Figure 11. Surface tension of suspension with respect to different concentration of amphiphiles.[4]

4.2. Air content and wet foam stability

The total porosity of directly foamed ceramics is proportional to the amount of air incorporated into the suspension or liquid medium during the foaming process. The pore size, on the other hand, is determined by the stability of the wet foam. High-volume foams are formed upon mechanical frothing which strongly indicates the stabilization of air bubbles due to the attachment of particles to the air-water interface.

In Fig. 12, a relationship between the air content and the different concentration of amphiphiles has been plotted. It can be seen that for all three amphiphiles, the air content gradually increases until it achieves the highest value. This is because the particles were not sufficiently hydrophobized below this concentration (i.e., 0.15 m/mol for propionic acid and 0.10 m/mol for valeric acid). All the investigated suspension reports highest air content (i.e., 69% in case of propionic acid and 58-60% in case of butyric acid and valeric acid) upon achieving sufficient hydrophobization. The decrease in air content at high amphiphile concentration is due to increase of suspension viscosity which resists the air incorporation to the suspension.

In Fig. 13, the influence of the amphiphile concentration on the wet foam stability is displayed. At very low amphiphile concentrations, no stable foams are obtained since the alumina particles are not sufficiently hydrophobized to stabilize the air-water interface of freshly formed air bubbles. Using 0.10 mol/L of amphiphile results in rather unstable foam with wet foam stability of about 72-77%. At a certain point between 0.15 and 0.2 mol/L of amphiphile concentration, wet foams with highest stability are obtained. Propionic acid having the shortest

hydrophobic chain requires more concentration (0.20 mol/L) to result sufficient hydrophobization. However, the middle and long chain amphiphiles, i.e., butyric acid and valeric acid, respectively, produce effective hydrophobicity at around 0.15 mol/L. More concentrations of them increase the suspension viscosity results from increasing hydrophobicity of the particles, which prohibits the suspension to be foamed by mechanical stirring.

Fig. 14 establishes the air contents and foam stability of Al_2O_3-TiO_2equimolar suspension, with respect to different vol% of 3:2 mole ratio of Al_2O_3-SiO_2 suspension added for the mullite phase. High-volume foams with air content up to 83% form upon mechanical frothing, which strongly indicates the stabilization of air bubbles, due to the attachment of particles to the air-water interface. We measured the foam stability and observed that on the addition of 10 vol% suspension for the mullite phase, the foam stability suddenly decreased. This is probably due to the high viscosity of the suspension, due to higher particle concentration. However, 20, 30, and 50 vol.% of addition enhanced the foam stability, which might be explained by the optimum surface hydrophobicity being achieved, due to the increased particle concentration.

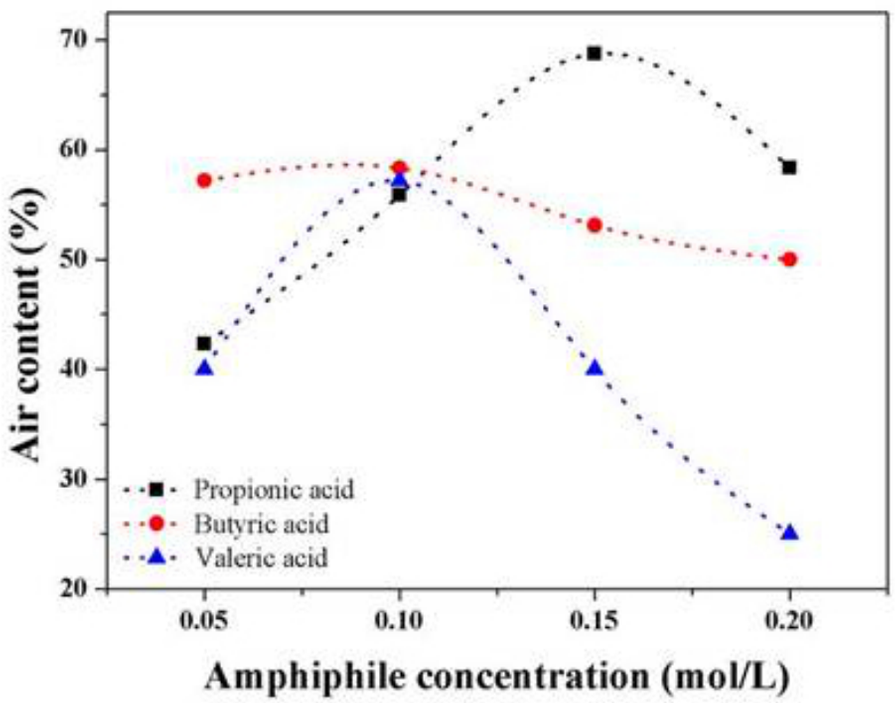

Figure 12. Air content of suspension with respect to different concentration of amphiphiles.[4]

In Fig. 15, the wet foam stability can be determined by observing the average bubble size with respect to the time after foaming. The foams stabilized with butyric acid and valeric acid show no significant bubble growth unlike the foam stabilized with propionic acid which shows a little coarsening. We can attribute the first two cases of remarkable resistance to the irreversible adsorption of the partially hydrophobized particles at the air-water interface. Therefore, the bubble size remains almost constant with the increase of time up to 6 hours of foaming. The foams stabilized with propionic acid are prone to bubble coarsening due to the pressure

http://dx.doi.org/10.5772/61047

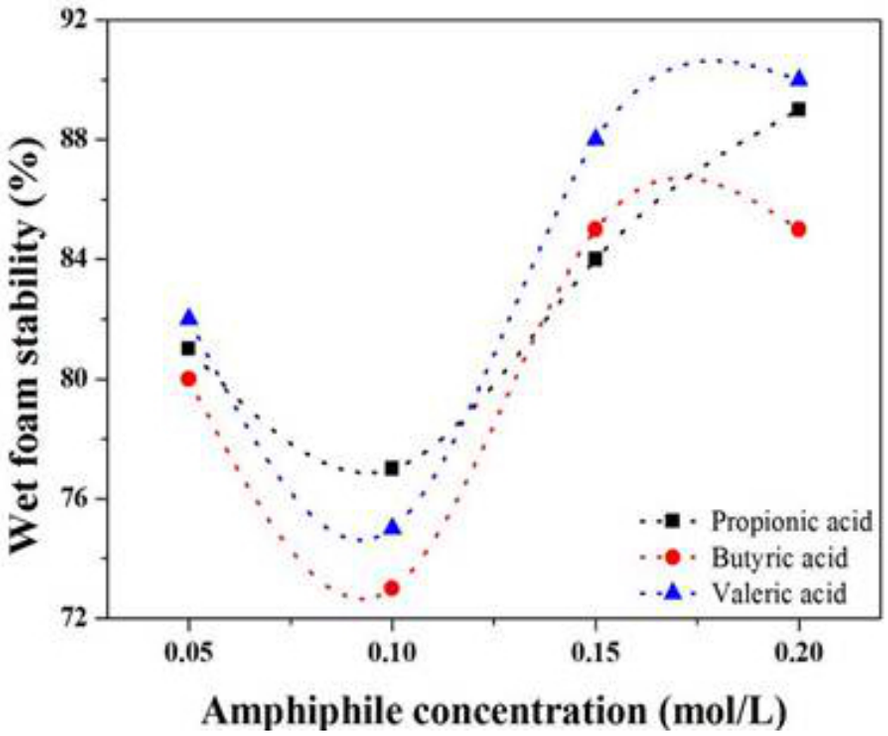

Figure 13. Wet foam stability of suspension with respect to different concentration of amphiphiles.[4]

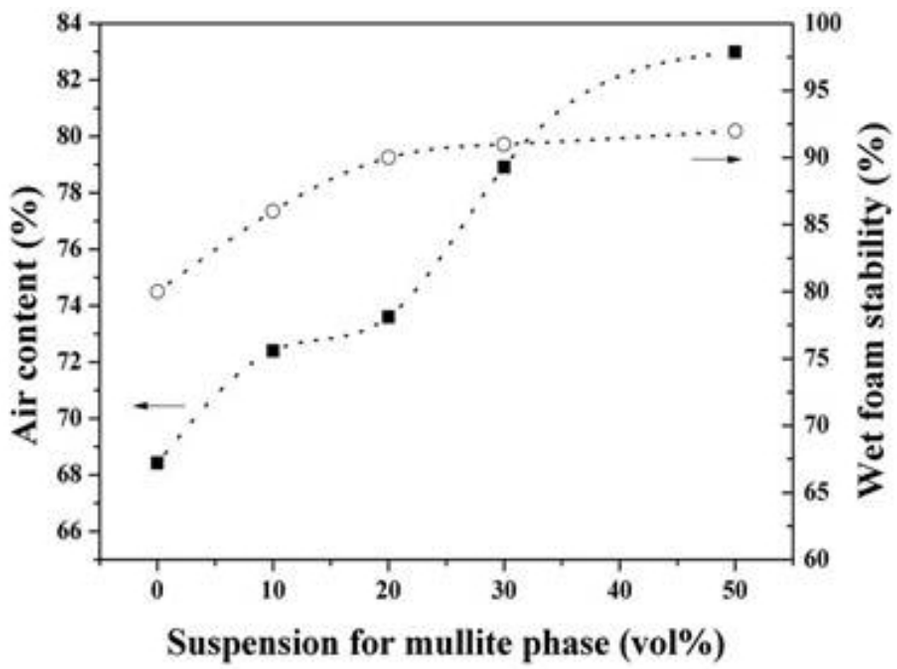

Figure 14. Air content and foam stability of Al_2O_3-TiO_2equimolar suspension, with respect to different vol% of 3:2 mole ratio of Al_2O_3-SiO_2 suspension added for the mullite phase.[32]

difference between two bubbles of different radius which leads to Ostwald ripening. This thermodynamically driven spontaneous process occurs because the internal pressure of a

particle is indirectly proportional to the radius of the particle. Large particles, with their lower surface to volume ratio, result in a lower energy state, whereas the smaller particles exhibit higher surface energy. As the system tries to lower its overall energy, molecules on the surface of a small particle tends to detach. It diffuses through colloidal solution and attaches to the surface of larger particle. Therefore, the number of smaller particles continues to shrink, while larger particles continue to grow [17].

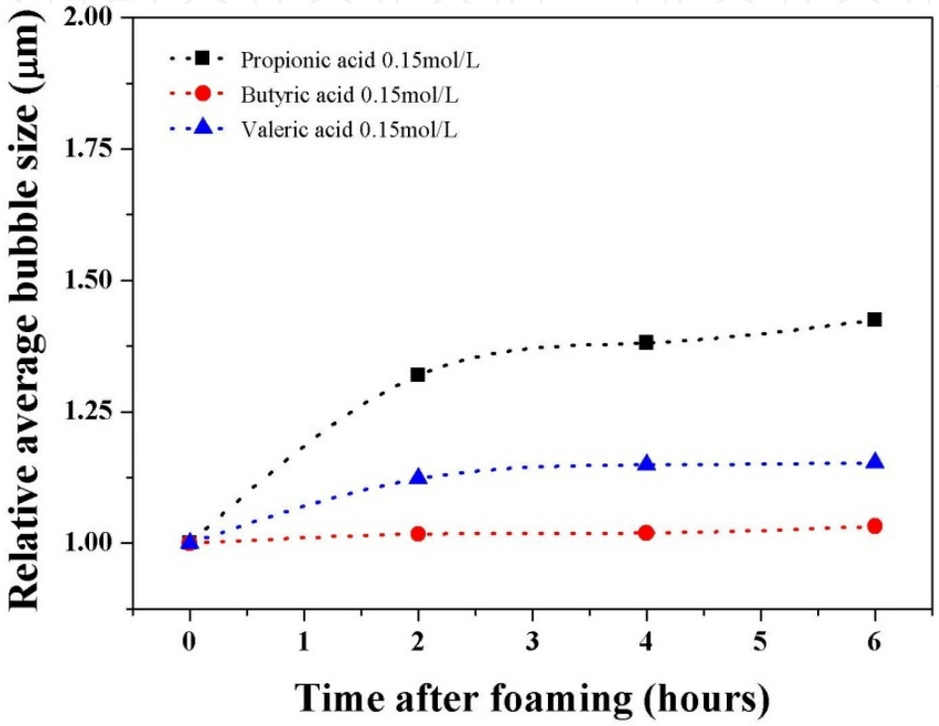

Figure 15. Relative average bubble size of suspension with respect to time after foaming.[4]

4.3. Adsorption free energy

The adsorption free energy plays an important role in stabilizing foams. Particles attached to the gas-liquid interfaces of foams lower the system free energy, by replacing part of the gas-liquid interfacial area. According to Equation (1), G (the Gibbs free energy) is greatest when θ is 90º; however, the foam stabilization of particles readily occurs when θ is between 50º and 90º.

Fig. 16 shows the change in the adsorption energy corresponding to the different mole ratio of SiO_2 content used to stabilize the suspension.An Al_2O_3 loading of 30 vol.% in the suspension was taken as a standard, and experiments were performed with 0.01 mol L^{-1} amphiphiles for stabilization of the particles. The calculations show that the energy level decreases with the nanoparticle size and with increase in SiO_2 content. However, after the middle value (0.75) of the SiO_2 loading, the van der Waals attraction force between the particles gradually increases, forcing the suspension to destabilize and finally decrease the wet foam stability from 87% to

http://dx.doi.org/10.5772/61047

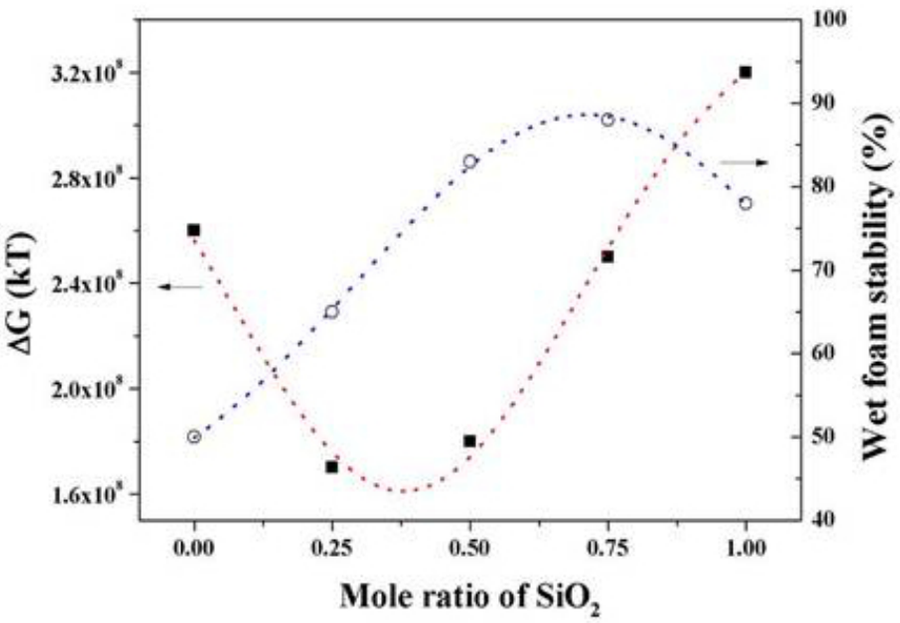

Figure 16. Free energy and wet foam stability with respect to the different mole ratio of SiO_2.

68%. A higher energy of adsorption of 1.7×10^8 kTs could be achieved in the initial suspension without SiO_2 content. The adsorption free energy decreases with the increasing concentration. Higher contact angle of 62°-75° with a lower interfacial energy of 1.7×10^8 kTs were seen at SiO_2 mole ratio of 0.25 giving an interfacial tension of 42-45 mNm^{-1}.

Fig. 17 establishes the relationship between adsorption free energy corresponding to the foam stability, with respect to the different vol.% of suspension added for the mullite phase. Low adsorption free energy resulting from the spontaneous bubble growth leads to foam instability. The investigated samples exhibit much higher adsorption free energy of about 2.2×10^{-13} J to 2.7×10^{-13} J at the interface, resulting in irreversible adsorption of particles at the air-water interface, which leads to outstanding stability.

In Fig. 18, a relationship between adsorption free energy corresponding to the concentrations of different chain length of amphiphile has been established. Stable and unstable zones have been described relating to the data obtained by the wet foam stability graph. Low adsorption free energy (e.g., 2.05×10^{-13} J to 3.78×10^{-13} J) results from the spontaneous bubble growth leads to foam instability. However, higher adsorption free energy of about 4.52×10^{-13} J to 8.22×10^{-13} J at the interface results in irreversible adsorption of particles at the air-water interface which leads to outstanding stability.

4.4. Laplace pressure and bubble size

Fig. 19 shows the wet foam stability corresponding to the pressure exerted by the bubbles (Laplace pressure) with respect to the different mole ratio of SiO_2 content. The Laplace pressure increases with the increase in SiO_2 concentration. This behavior can be attributed to the fact that high silica content requires a large volume of water in the suspension, which subsequently

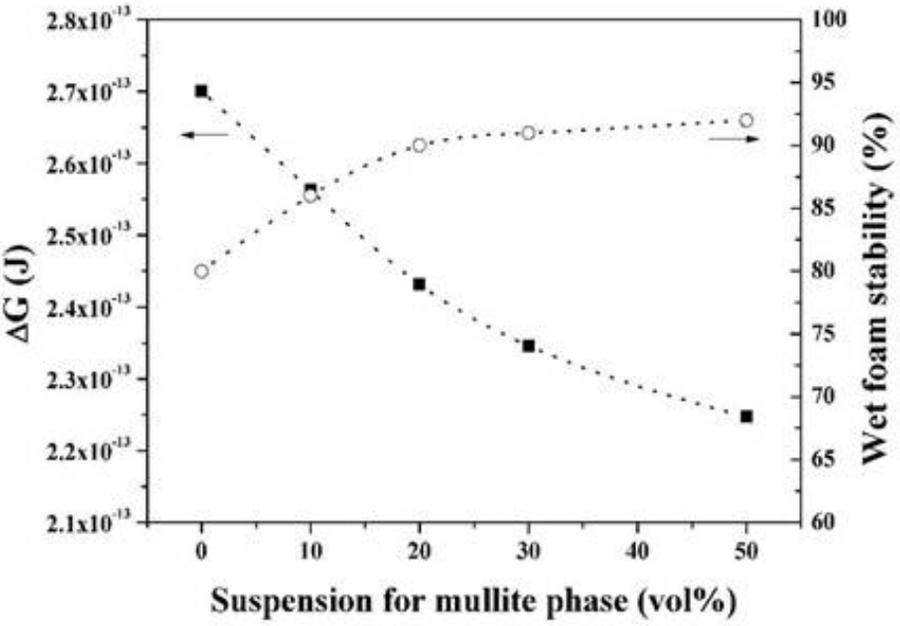

Figure 17. Adsorption free energy and foam stability of Al_2O_3-TiO_2 equimolar suspension, with respect to different vol % of 3:2 mole ratio of Al_2O_3-SiO_2 suspension added for the mullite phase.[32]

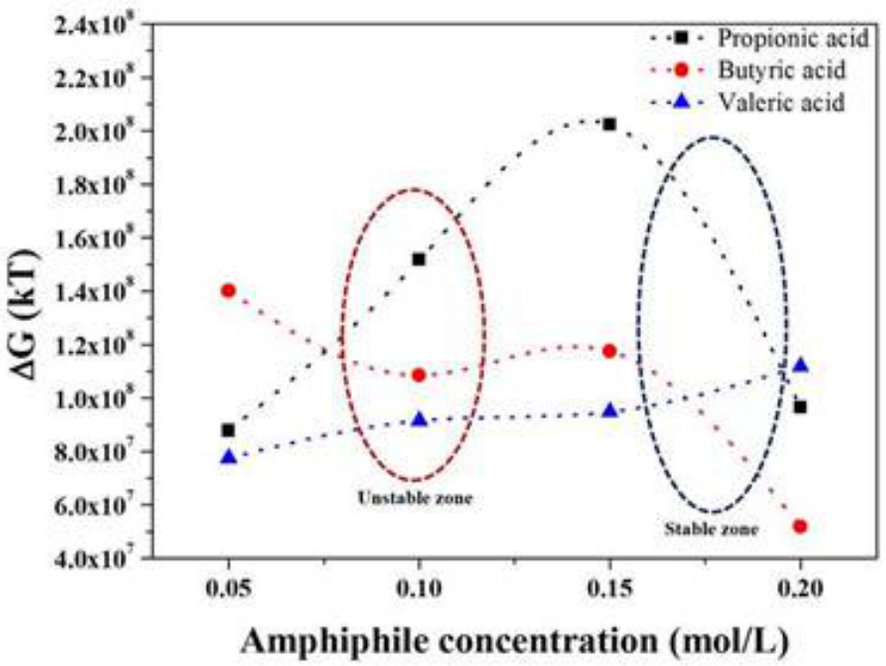

Figure 18. Adsorption free energy of suspension with respect to different concentration of amphiphiles.[4]

lowers the outer pressure of the bubble. The wet foam stability suddenly decreases due to high Laplace pressure when the mole ratio of SiO_2 reached at 0.60. The wet foams were stable at the pressure difference between 20 and 25 mPa, which corresponds to the SiO_2 mole ratio content of 0.25-0.50. The stability increased to more than 80% at a SiO_2 mole ratio of 0.75.

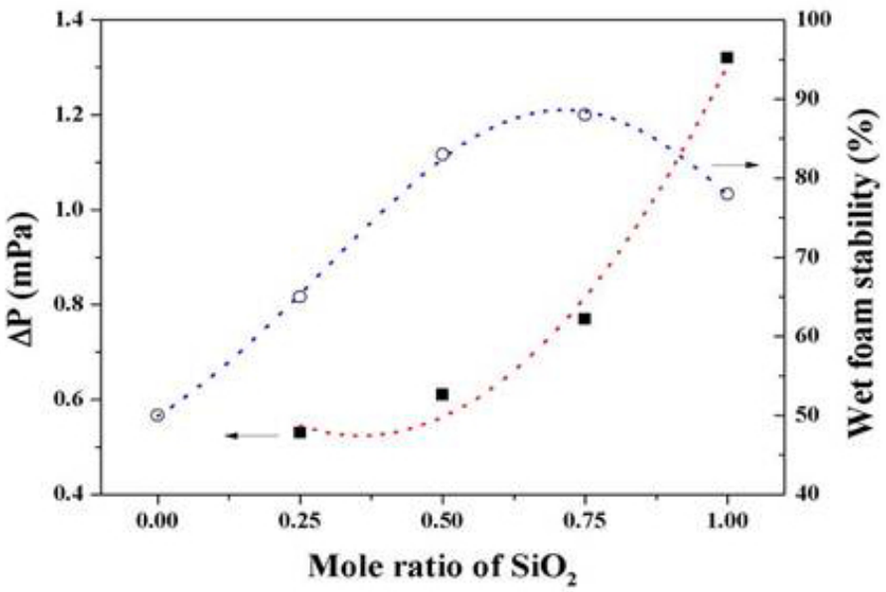

Figure 19. Laplace pressure and wet foam stability with respect to the different mole ratio of SiO_2 content.

Fig. 20 plots the graph of the Laplace pressure and average bubble size of all evaluated suspensions, with respect to the various vol.% of suspension for the mullite phase. As we can see, instability occurs when the Laplace pressure is too low. Wet foam stability occurs when the Laplace pressure is about 1.5-2.2 mPa. The degree of particle hydrophobization influences the average bubble size of the resultant foams. Fig. 20 shows that the average bubble size decreases with increasing particle concentration and particle hydrophobicity. This is due to the decrease in surface tension and increase in foam viscosity that result from higher particle concentrations. This reduces the resistance of air bubbles against rupture and thus leads to the production of foams with average bubble sizes.

In Fig. 21, the Laplace pressure of all evaluated suspensions has been plotted in a graph with respect to the various concentration of different chain length of amphiphile. As we can see, the instability occurs when the Laplace pressure is too low as in case of 0.10 mol/L of amphiphile concentration. Wet foam stability occurs when Laplace pressure is about 0.8-1.4 mPa. Valeric acid, having the longest chain length, exhibits high Laplace pressure resulting in outstanding stability of wet foam.

The degree of particle hydrophobization, which is directly related to the concentration of amphiphile, influences the average bubble size of the resultant foams. Fig. 22 shows the bubble size of the suspension and the pore size by thin film or struts formed after the foaming of the particle stabilized suspension and sintering. The average bubble size for these types of stabilized foams was 98-140 μm. The required partial hydrophobization of the particles occurs at this point, which leads to porous ceramics with porosity greater than 80% and pore size of about 108 μm after sintering at 1300°C for 1 hour.

In Fig. 23, it can be seen that the average bubble size decreases with increasing amphiphile concentration and particle hydrophobicity. This is due to the decrease in surface tension and

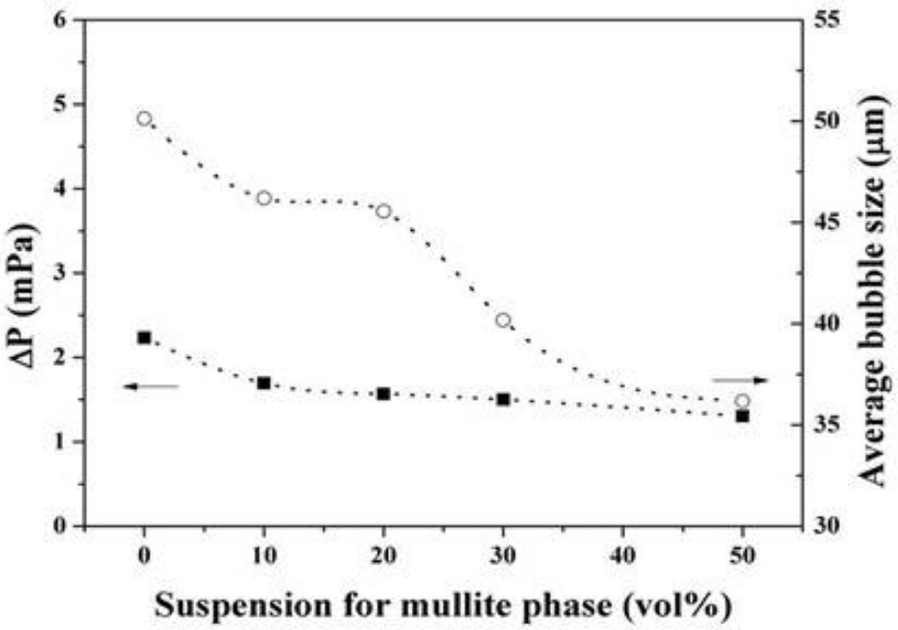

Figure 20. Laplace pressure and bubble size of Al_2O_3-TiO_2 equimolar suspension, with respect to different vol% of 3:2 mole ratio of Al_2O_3-SiO_2 suspension added for the mullite phase.[32]

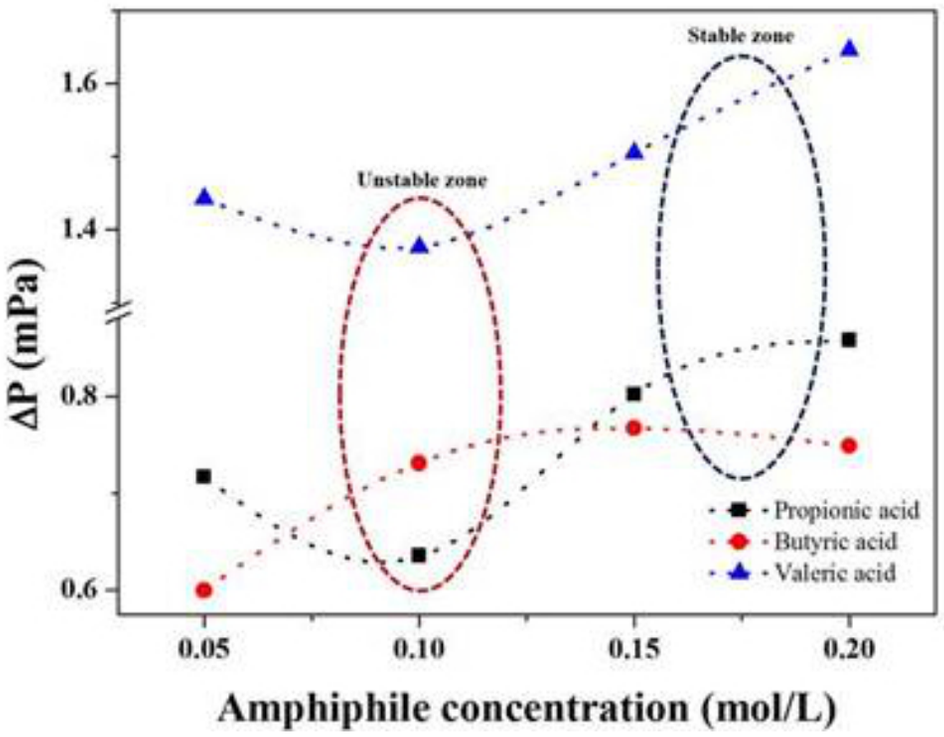

Figure 21. Laplace pressure of suspension with respect to different concentration of amphiphiles.[4]

increase in foam viscosity because of higher amphiphile concentrations. This decreases the resistance of air bubbles against rupture and thus leads to produce foams with average bubble sizes. It is interesting to note that valeric acid, having the longest amphiphilic chain, produces

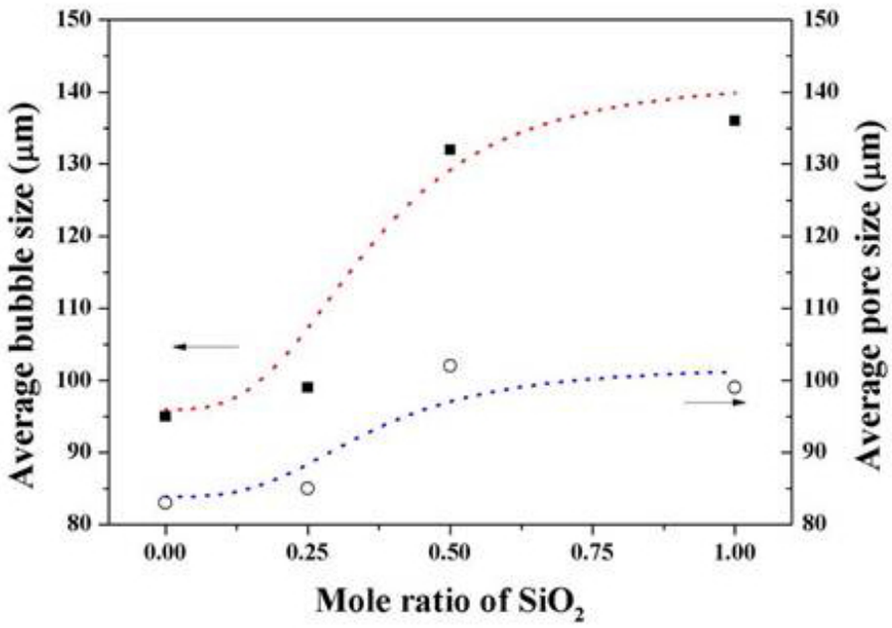

Figure 22. Bubble size and pore size with respect to the SiO_2 content of the wet foam before and after sintering at 1300°C for 1 hour.

very small sized bubbles of about 35-25 μm. This can be attributed to the greater hydrophobicity, which results in enhanced stability of particle stabilized foams against bubble coalescence and Ostwald ripening [see Fig. 26(c)].

4.5. Microstructure analysis

The microstructures are described in Fig. 24, where tailored, open and closed, interconnected pores can be seen. Also, it can be seen that the larger and smaller pores are uniformly distributed. In Fig. 24a-d, different compositions of Al_2O_3/SiO_2 with well-developed and narrow pore size distribution can be seen. It shows a hierarchical pore distribution with porosities up to 80% from larger to smaller pores and thick struts (films in wet foams). It leads to produce more stable foams sintered to form porous ceramics with high mechanical strength.

Fig. 25 shows the microstructures of porous (a) AT, (b) ATM1, (c) ATM3, and (d) ATM5, sintered at 1500°C for 1 hour. The microstructures obtained generally consist of open, interconnected pores with a narrow pore size distribution. The composition without addition of mullite (Fig. 25(a)) shows the characteristic microstructure of Al_2TiO_5: an open porous and microcracked Al_2TiO_5 matrix phase, with the presence of abnormal grain growth. These grains can be attributed to unreacted Al_2O_3 and TiO_2 due to the formation reaction kinetics, which is a process led by the nucleation and growth of Al_2TiO_5 grains, and finally the diffusion of the reactants through the matrix. It is evident from Fig. 25b-d that the addition of mullite has a beneficial effect on grain growth control.

The scanning electron microscope images of 30 Vol% Al_2O_3-SiO_2 porous ceramics sintered at 1300°C with different chain length amphiphile of concentration 0.15 mol/L are shown in Fig. 26. The microstructures obtained are generally consists of closed pores. It is interesting to note

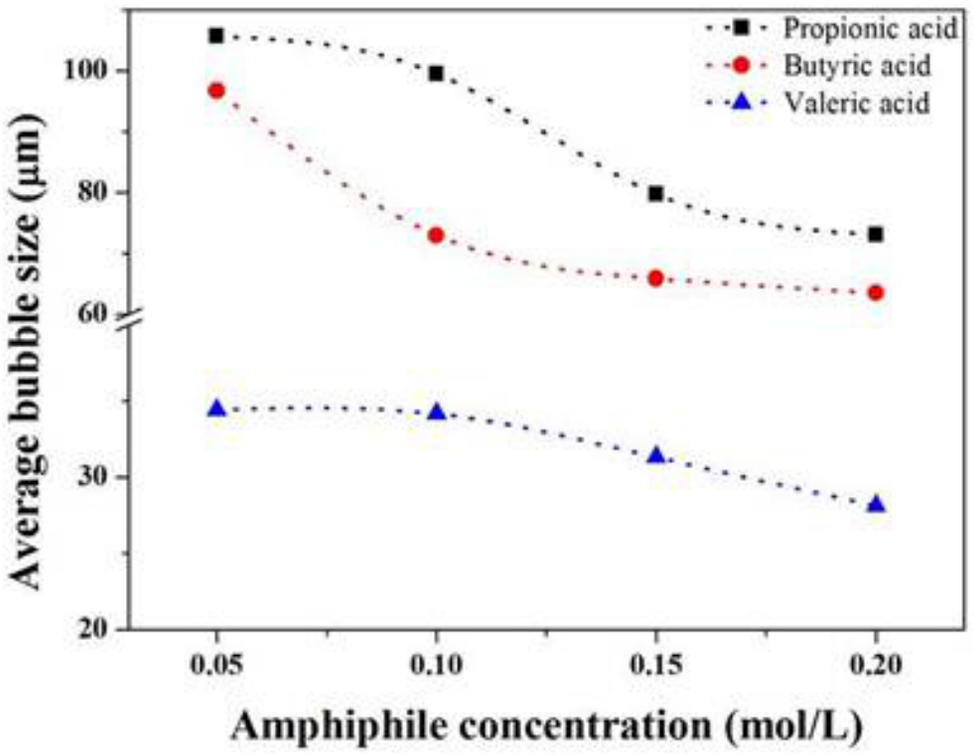

Figure 23. Average bubble size of suspension with respect to different concentration of amphiphiles.[4]

that at the same concentration of amphiphile, the shortest chain carboxylic acid, i.e., propionic acid, produces relatively large pore size than the longest chain carboxylic acid, i.e., valeric acid. This can be attributed to the fact that greater hydrophobicity is achieved with the aid of long carbon chain present in valeric acid which results in small and uniform pore size. The smaller cell sizes result from the high stability of the foams in the wet state, which impedes bubble coarsening. The dense struts as shown in the inset of Fig. 26a-c plays vital role for improving the mechanical strength of the porous ceramics.

5. Conclusions

Porous ceramics' microstructures and properties are affected by their method of synthesis. Direct foaming can simply, inexpensively and quickly prepare macroporous ceramics. Open or closed porosities of 45%-85% having been demonstrated. The pores produced by this method result from the direct incorporation of air bubbles into a ceramic suspension, eliminating the need for pyrolysis before sintering. Cellular structures prepared by direct foaming are generally stronger than those prepared by replica synthesis due mainly to the absence of flaws in the cell struts. Given the importance of the chosen synthetic method, this review examines currently available processes for forming porous ceramics. Direct foaming is a simple and versatile process for the low-cost manufacture of porous ceramics for various applications. Its continuous study will result in further improvements of its method and wider applicability

http://dx.doi.org/10.5772/61047

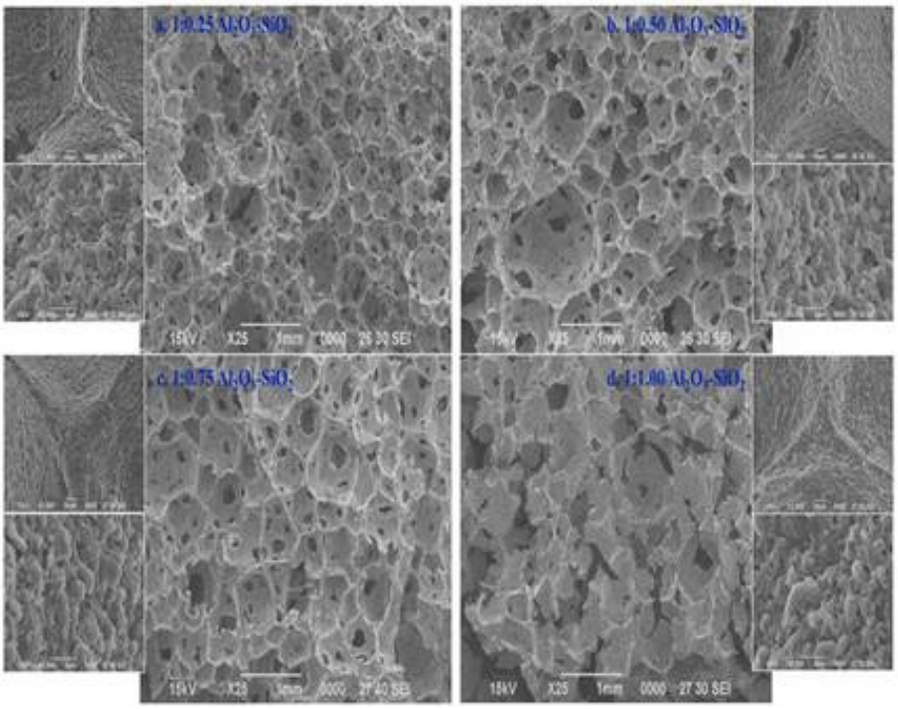

Figure 24. Microstructures and thin film (inner cell) of porous ceramics sintered at 30 vol.% Al_2O_3 with respect to the different mole ratio of SiO_2 content.

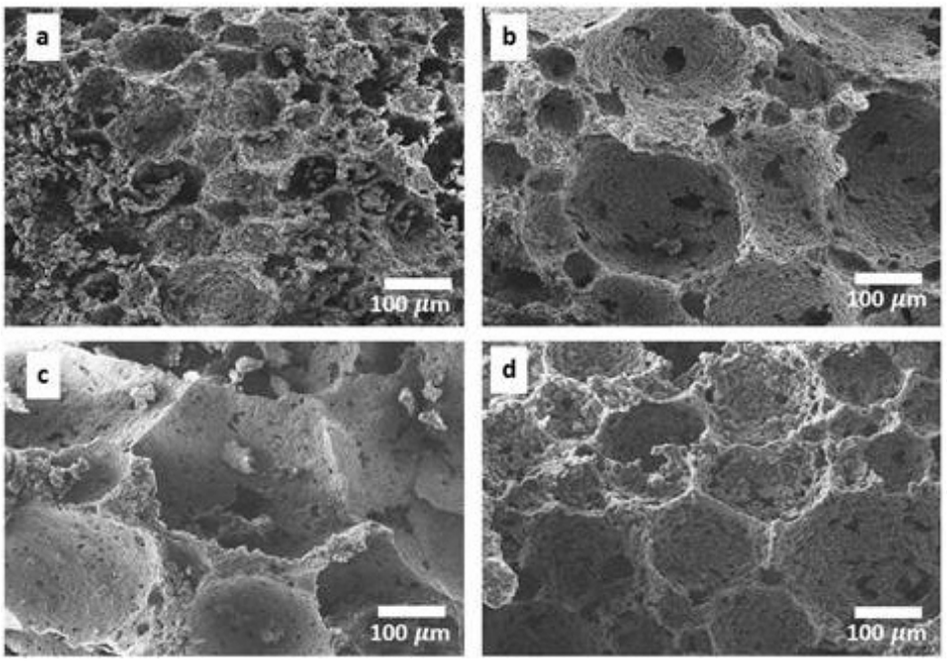

Figure 25. Microstructures of (a) AT, (b) ATM1, (c) ATM3, and (d) ATM5 porous ceramics, sintered at 1500°C for 1 hour.[32]

of its products. Examination of the literature led to the proposal of an equation describing the inverse proportionality of wet foam stability to the surface of the liquid-air interface.

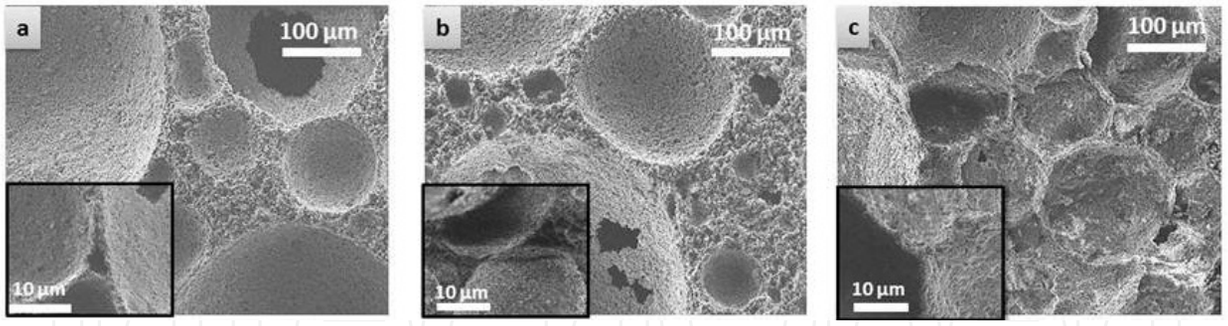

Figure 26. Microstructures of porous ceramics using 0.15 mol/L of (a) propionic acid, (b) butyric acid, and (c) valeric acid; the inset in (a), (b), and (c) show single dense struts obtained with direct foaming method.[4]

$$W_{fS} \infty (\frac{1}{\gamma})$$

W_{fS} = Wet foam stability

γ = surface tension

Acknowledgements

This research was financially supported by the Ministry of Education, Science Technology (MEST), and The National Research Foundation of Korea (NRF) through the Human Resource Training Project for Regional Innovation and Hanseo University.

Author details

Naboneeta Sarkar and Ik Jin Kim*

*Address all correspondence to: ijkim@hanseo.ac.kr

Department of Materials Science and Engineering, Institute of Processing and Application of Inorganic Materials (PAIM), Hanseo University, # , Haemi-myun, Daegok-ri, Seosan-city, Chungnam, South Korea

References

[1] M. Scheffler and P. Colombo, Cellular Ceramics: Structure, Manufacturing, Properties and Applications. p 645. Weinheim, Wiley-VCH, 2005.

[2] A. R. Studart, U. T. Gonzenbach, E. Tervoort, and L. J. Gauckler, "Processing routes to macroporous ceramics—a review," J. Am. Ceram. Society (2006).

[3] J. Banhart, "Manufacturing Routes for Metallic foams," JOM (2000).

[4] N. Sarkar, J. G. Park, S. Mazumder, A. Pokhrel, C. G. Aneziris, and I. J. Kim, Effect of amphiphile chain length on wet foam stability of porous ceramics, Ceram. Int., 41 [3] (2015) 4021-4027.

[5] J. Banhart, "Manufacture, classification and application of cellular metals and foams," Prog. Mater. Sci., 46 (2001) 559-632.

[6] W. Ramsden, "Separation of solids in the surface-layers of solutions and 'suspensions'," Proc. R. Soc. Lond., 72 (1903) 156.

[7] Ya. Guzman, "Certain principles of formation of porous ceramic structures, properties and applications—a review," Glass Ceram., 9 (2003) 28-31.

[8] P. Colombo and J.R. Hellmann, "Ceramic foams from preceramic polymers," Mat Res. Innovat., 6 (2002) 260-272.

[9] H. M. Princen and A. D. Kiss, "Rheology of foams and highly concentrated Emulsions," J. Colloid. Interface Sci., 128 [1] (1989) 176-187.

[10] W. D. Kingery, H. K. Bowen, and D. R. Uhlmann, Introduction to Ceramics, 2nd edition. Wiley Interscience Publication, 1975.

[11] P. Colombo, "Conventional and novel processing methods for cellular ceramics," Phil. Trans. R. Soc. A., 364 (2006), 109-124.

[12] B. Neirinck, J. Fransaer, O. V. der Biest, JefVleugels, "A novel route to produce porous ceramics," J. Euro. Cerm. Soc., 29 (2009) 833-836.

[13] B. P. Binks, "Particles as surfactants—similarities and differences," Curr. Opin. Colloid Interface Sci., 7 (2002) 21-41.

[14] Brent S. Murray, "Stabilization of bubbles and foams," Curr. Opin. Colloid Interface Sci., 12 (2007) 231-241.

[15] T. S. Horozov, "Foams and foam films stabilized by solid particles," Curr. Opin. Colloid Interface Sci., 13 (2008) 134-140.

[16] P. C. Hidber, T. J. Graule, and L. J. Gauckler, "Influence of the dispersant structure on properties of electrostatically stabilized aqueous alumina suspension," J. Eur. Ceram. Soc., 17 [2-3] (2002) 239-249.

[17] A. Pokhrel, J. G. Park, J. S. Nam, D. S. Cheong, and I. J. Kim, "Stabilization of wet foams for porous ceramics using amphiphilic particles," J. Kor. Ceram. Soc., 48 [5] (2011) 463-466.

[18] N. D. Denkov, I. B. Ivanov, P. A. Kralchevsky, and D. T. Wasan, "A possible mechanism of stabilization of emulsions by solid particles," J. Colloid. Interface Sci., 150, [2] (1992) 589-593.

[19] L. J. Gauckler, Th. Graule, and F. Baader, "Ceramic forming using enzyme catalyzed reactions," Mater. Chem. Phys., 61 (1999) 78-102.

[20] A. Pokhrel, Zhao Wei, and I. J. Kim, "Wet foam stabilized by amphiphiles to tailor the microstructures of porous ceramics," Key Eng. Mater., 512-515 (2012) 288-292.

[21] A. B. Subramaniam, C. Mejean, M. Abkarian, and H. W. Stone, "Microstructure, morphology and lifetime of armored bubbles exposed to surfactants," Langmuir, 22 [14] (2006) 5986-5990.

[22] U. T. Gonzenbach, A. R. Studart, D. Steinlin, E. Tervoort, and L. J. Gauckler, "Processing of particle-stabilized wet foams into porous ceramics," J. Am. Ceram. Soc., 90 [11] (2007) 3407-3414.

[23] U. T. Gonzenabach, A. R Studart, E. Tervoort, and L. J. Gauckler, "Stabilization of foams with inorganic colloidal particles," Langmuir, (2006) 10983-10988.

[24] T. N. Hunter, R. J. Pugh, G. V. Fanks, and G. J. Jameson, "A role of particles in stabilizing foams and emulsions," Adv. Colloid. Inter. Sci., 137 (2008) 57-81.

[25] U. T. Gonzenbach, A. R. Studart, E. Tervoort, and L. J. Gauckler, "Macroporous ceramics from particle-stabilized wet foams," J. Am. Ceram. Soc., 90 [1] (2007) 19-22.

[26] P. J.Wilde, "Interface: their role in foam and emulsion behavior" Curr. Opin. Colloid Interface Sci., 5 (2000) 176-181.

[27] G. Morris, M. R. Pursell, S. J. Neethling, and J. J. Cilliers, "The effect of particle hydrophobicity, separation distance and packing patterns on the stability of a thin film," J. Colloid Interface Sci., 327 (2008) 138-144.

[28] U. T. Gonzenbach, A. R. Studart, E. Tervoort, and L. J. Gauckler, "Tailoring the microstructure of particle-stabilized wet foams," Langmuir, 23[3] (2007) 1025-1032.

[29] I. Akartuna, A. R. Studart, E. Tervoot, U. T. Gonzenbach, and L. J. Gauckler, "Stabilization of oil-in-water emulsions by colloidal particles modified with short amphiphiles," Langmuir, 24 (2008) 7161-7168.

[30] A. R. Studart, U. T. Gonzenbach, I. Akartuna, E. Tervoort, and L. J. Gauckler, "Materials from foams and emulsions stabilized by colloidal particles," J. Mater. Chem., (2007) 3283-3289.

[31] A. Pokhrel, J. G. Park, G. H. Jho, J. Y. Kim, and Ik Jin Kim, "Controlling the porosity of particle stabilized Al_2O_3 based ceramics," J. Kor. Ceram. Society., 48 [6] (2011) 600-603.

[32] N. Sarkar, J. G. Park, S. Mazumder, A. Pokhrel, C. G. Aneziris, and I. J. Kim, "Al_2TiO_5-mullite porous ceramics from particle stabilized wet foam," Ceram. Int., 41 [5] (2015) 6306-6311.

[33] I. Aranberri, B. P. Binks, J. H. Clint, and P. D. I. Fletcher, "Synthesis of macroporous silica from solid-stabilised emulsion templates," J. Porous. Mater.,16 (2009) 429-437.

[34] U. T. Gonzenabach, A. R Studart, E. Tervoort, and L. J. Gauckler, "Ultrastable particle-stabilized foams," Angew. Chem. Int. Ed., 45 (2006) 3526-3530.

[35] E. Dickinson, R. Ettelaie, T. Kostakis, and B. S. Murray, "Factors controlling the formation and stability of air bubbles stabilized by partially hydrophobic silica nanoparticles," Langmuir, 20 (2004) 8517-8525.

[36] T. Fukasawa and M. Ando, "Synthesis of porous ceramics with complex pore structure by freeze-dry processing," J. Am. Ceram. Soc., 84 [1] (2001) 230-232.

[37] T. Fukasawa, Z. Y. Deng, M. Ando, T. Ohji, and Y. Goto, "Pore structure of porous ceramics synthesized from water-based slurry by freeze-dry process," J. Mater. Sci., 36 (2001) 2523-2527.

[38] I. Akartuna, A. R. Studart, E. Tervoot, and L. J. Gauckler, "Macro porous ceramics from particle-stabilized emulsions," Adv. Mater., 20 (2008) 4714-4718.

[39] I. Akartuna, E. Tervoot, A. R. Studart, and L. J. Gauckler, "General route for the assembly of functional inorganic capsules," Langmuir 25[21], (2009) 12419-12424.

[40] A. Pokhrel, J. G. Park, W. Zhao, and I. J. Kim, "Functional porous ceramics using amphiphilic molecule," J. Ceram. Process. Res., 13 [4] (2012) 420-424.

[41] Brent. S. Murray and Ettelaie, "Foam stability: proteins and nanoparticles," Curr. Opin. Colloid Interface Sci., 9 (2004) 314-320.

[42] D. M. Alguacil, E. Tervoort, C. Cattin, and L. J.Gauckler, "Contact angle and adsorption behavior of carboxylic acids on α-Al_2O_3 surfaces," J. Colloid Interface Sci., 353 (2011) 512-518.

[43] G. Kaptay, "On the equation of the maximum capillary pressure induced by solid particles to stabilize emulsions and foams and on the emulsion stability diagrams," Colloids Surf. A: Physicochem. Eng. Aspects., 282-283 (2006) 387-401.

[44] S. Barg, C. Soltmann, M. Andrade, D. Koch, and G. Grathwohl, "Cellular ceramics by direct foaming of emulsified ceramic powder suspensions," J. Am. Ceram. Soc., 91 [9] (2008) 2823-2829.

[45] C. Tuck and J. R. G. Evans, "Porous ceramics prepared from aqueous foams," J. Mater. Sci. Lett., 18 (1999) 1003-1005.

[46] F. Schuth and W. Schmidt, "Microporous and mesoporous materials" Adv. Eng. Mater., 4 [5] 92005) 269-279

[47] A. R. Studart, R. Libanori, A, Moreno, U. T. Gonzenbach, E. Tervoort, and L.J. Gauckler, "Unifying model for the electrokinetic and phase behavior of aqueous suspensions containing short and long amphiphiles," Langmuir, 27 (2011) 11835-11844.

[48] J. C. H. Wong, E. Tervoort, S. Busato, Urs. T. Gonzanbech, A. R. Studart, P. Ermanni, and L. J. Gauckler, "Designing macro porous polymers from particle-stabilized foams," J. Mater. Chem., 20 (2010) 5628-5640.

[49] A. R. Studart, Julia Studer, Lei Xu, K. Yoon, H. C. Shum, and D. A. Weitz, "Hierarchical porous materials made by drying complex suspensions," Langmuir, 27 [3] (2011) 955-964.

[50] P. C. Hiemenz and R. Ayagopalan, "Principles of colloid and surface chemistry," p. 650. 3rd edition. Marcel Dekker Inc, New York, 1997.

IntechOpen